

## Photoluminescence of CdSe quantum dots and rods from buffer-layer-assisted growth

V. N. Antonov, P. Swaminathan, J. A. N. T. Soares, J. S. Palmer, and J. H. Weaver<sup>a)</sup>  
*Department of Physics, Department of Materials Science and Engineering, Frederick Seitz Materials Research Laboratory, University of Illinois at Urbana-Champaign, Urbana, Illinois 61801*

(Received 15 November 2005; accepted 27 January 2006; published online 20 March 2006)

The traditional colloidal routes of fabrication of II-VI semiconductor quantum dots have been difficult to integrate with silicon technology. Here, we demonstrate that CdSe quantum dots and rods can be self-assembled and delivered in ultrahigh vacuum conditions on almost any substrate by means of buffer-layer-assisted growth (BLAG), where the buffer is thin solid Xe film. We determine the diffusivity of the particles on the buffer, and demonstrate the significance of the ionicity of the CdSe. Photoluminescence spectra are compared to the previous studies of colloidal CdSe structures. This study opens the door for the synthesis of tunable II-VI heterostructures. © 2006 American Institute of Physics. [DOI: 10.1063/1.2187411]

Nano-particles of II-VI semiconductors (quantum dots), which exhibit well-known size-dependent optical properties due to the quantum confinement of their charge carriers, have prospective uses in optoelectronic devices.<sup>1,2</sup> The principal routes of their synthesis have been chemical and thus difficult to integrate with existing silicon technology.<sup>3</sup> In most cases, substrates need to be robust to contamination, and the poor interface with the ligand-coated facets can result in clumping.<sup>4</sup> Moreover, the properties of any electrical interface with the dots could be significantly affected by the ligands.<sup>5</sup> In this work, we demonstrate that size-controlled CdSe quantum dots can be self-assembled under ultrahigh vacuum conditions, and controllably delivered on almost any substrate, by means of buffer-layer-assisted growth (BLAG). This is a general process, and it could easily be extended to other II-VI semiconductors.

In BLAG, physical vapor deposition of atoms on buffer layers of solid rare gases leads to the spontaneous formation of clusters. Subsequent warming causes both sublimation of the buffer and diffusion and aggregation of the clusters before their contact with the substrate.<sup>6</sup> The competition between buffer desorption and particle diffusion makes it possible to control the average size/density of these structures over more than three orders of magnitude as the extent of this aggregation is controlled by the thickness of the buffer. BLAG has been utilized for the synthesis of amorphous Ge nanoparticles on Si without a wetting layer.<sup>7</sup>

In the experiment discussed here, the substrates were either standard carbon-coated Cu grids for transmission electron microscopy (TEM) or Si or GaAs wafers covered *in situ* with 5 nm of ZnS for photoluminescence (PL) measurements. They were cooled to ~20 K by means of a closed-cycle helium refrigerator. Solid Xe layers were grown by dosing Xe through a leak valve to produce the necessary exposure on the samples. CdSe was subsequently deposited by thermal evaporation from a quartz crucible, where CdSe evaporated as a molecule. Following warm-up to room temperature, the wafers intended for photoluminescence (PL) measurements were overcoated with 20 nm of ZnS to protect

the CdSe particles from air exposure and to improve the intensity of the signal.<sup>8</sup>

TEM micrographs of CdSe nanoparticles grown through BLAG by 2 Å deposition of CdSe on Xe buffers ranging from 2 to 12 monolayers (ML) are shown in Fig. 1. Growth on 2 ML Xe resulted in the formation of compact clusters of ~2 nm diameter with a density of  $1 \times 10^{12} \text{ cm}^{-2}$ . The particle density on such thin buffers corresponds to the initial density following nucleation on a Xe buffer, and it reflects the diffusivity of adsorbed CdSe molecules on solid Xe(111).<sup>9</sup> Deposition of the same amount of CdSe on thicker buffers resulted in the diffusion of these initial clusters and their aggregation into short rods, Fig. 1(b), and extended ramified islands, Fig. 1(c), with a typical branch width of 3 nm. This branch width is generally associated with the critical size of the aggregating entities, above which the rate

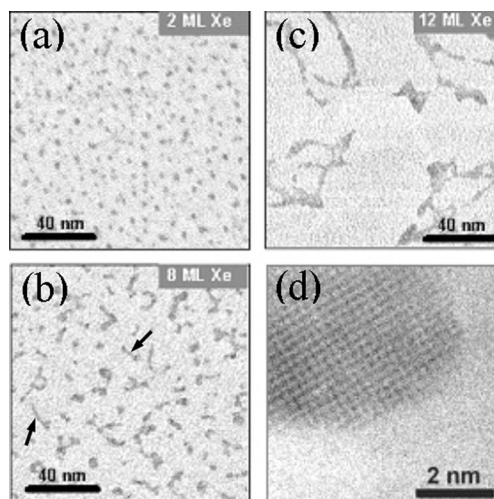


FIG. 1. (a)–(c) Bright-field TEM micrographs of CdSe nanoparticles on an amorphous carbon substrate, obtained from BLAG of 2 Å CdSe on solid Xe buffers of different thickness. Above 2 MLs, diffusion is activated and the dots aggregate into rods such as indicated by the arrows in (b). These rods are the early stages of the formation of extended ramified CdSe structures with ~3 nm branch width as in (c). The number density of the particles is reduced by more than two orders of magnitude between 2 and 18 ML Xe as aggregation occurs. (d) High-resolution TEM micrograph of a CdSe particle showing the cubic symmetry of the zinc-blende lattice.

<sup>a)</sup>Electronic mail: jhweaver@uiuc.edu

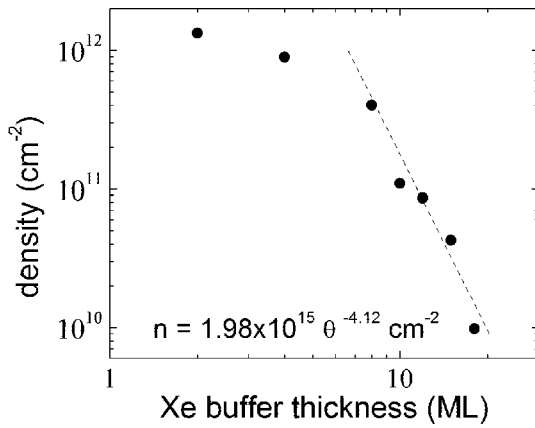


FIG. 2. Density of CdSe nanoparticles after 2 Å deposition and aggregation as a function of Xe buffer thickness. Competition between the exponential rates of particle diffusion and buffer desorption results in a power-law dependence from which the constants of particle diffusion on solid Xe are determined.

of particle-particle coalescence becomes smaller than the rate of particle-particle encounter.<sup>10</sup> This compares to a branch width of  $\sim 10$  nm for BLAG of metals,<sup>11</sup> and it reflects the slower rate of CdSe self-diffusivity. High-resolution TEM and electron diffraction show the zinc-blende phase of CdSe.

Figure 2 shows that the density of CdSe particles on the substrate exhibits a power-law dependence on the Xe buffer thickness, a result of the competition between the exponential increase with temperature of the particle diffusion rates and the Xe sublimation rate.<sup>9</sup> The power-law fit in Fig. 2 yields  $n = 1.98 \times 10^{15} \theta^{-4.12}$ , where  $n$  is the area density and  $\theta$  is the buffer thickness in ML. Thus BLAG of CdSe is qualitatively similar to BLAG of the metals studied previously.<sup>11</sup> Consequently, we can use the formalism developed earlier for the analysis of metal particle aggregation to obtain the constants of diffusion. Following Ref. 11, we calculate an effective activation energy for diffusion of  $1.09 \pm 0.16$  eV for the ramified CdSe islands, a value that is approximately twice what has been observed for metallic nanostructures.<sup>11</sup> While the contribution of the London dispersion forces to the binding energy of Xe on CdSe is not known, the polarizability per atom of the CdSe particle is in the range of  $4.3\text{--}4.4 \text{ \AA}^3$ .<sup>12</sup> This is comparable to that of the metals we studied previously (Ref. 11) (e.g.,  $\alpha_{\text{Cu}} = 6.1 \text{ \AA}^3$ ,  $\alpha_{\text{Pd}} = 4.8 \text{ \AA}^3$ ),<sup>13</sup> and thus we expect a London dispersion force of similar strength.

The higher effective barrier can be explained by the highly polar character of the Cd–Se bond and the existence of permanent dipoles on the CdSe particle surface that add to the CdSe–Xe van der Waals interaction. We can estimate the magnitude of the additional CdSe–Xe binding energy ( $U$ ) by considering the interaction between the induced dipole of a Xe atom ( $p_{\text{Xe}}$ ) and the field ( $E$ ) of the nearest permanent Cd–Se dipole on the surface of a CdSe particle. After Ref. 14,

$$U = -\frac{1}{2} \mathbf{p}_{\text{Xe}} \cdot \mathbf{E} = -\frac{1}{2} \alpha_{\text{Xe}} \frac{p_{\text{CdSe}}^2}{(4\pi\epsilon_0)^2 r^6} [1 + 3 \cos^2(\theta)], \quad (1)$$

where  $\theta$  is the angle of the dipole with respect to the dipole-atom direction,  $\alpha_{\text{Xe}} = 4\pi\epsilon_0 \times 4.044 \text{ \AA}^3$  is the polarizability of a Xe atom,<sup>13</sup>  $p_{\text{CdSe}}$  is the CdSe molecular dipole moment. The latter can be estimated from the effective Coulomb

charge determined as  $\pm Zf_i^{1/2}$ ,<sup>15</sup> where  $Z$  is the bond valence and  $f_i = 0.70$  is the Phillips ionicity for CdSe.<sup>16</sup> Averaging over  $\theta$  while keeping the inter-atomic distance at  $\sim 3 \text{ \AA}$  yields  $U \sim 0.2$  eV, which is comparable with the binding energies of a Xe adatom on metals [e.g., 0.21 eV for Xe/Au(111) or Ag(111), 0.27 eV for Xe/Pd(100)],<sup>17</sup> where the on-top adsorption sites are preferred.<sup>18</sup> This suggests that the contribution to the binding energy between Xe and CdSe due to the Xe-dipole interaction is comparable to the binding energy of Xe on metals due to dispersion forces alone, and a commensurate contribution to the cluster effective diffusion barrier is expected. It is therefore reasonable to expect that the increase of the effective diffusion barrier of the CdSe particles as compared to metals, such as Au, Co, and Pd, is due to the additional Xe-atom-permanent CdSe dipole interaction. We predict that effective diffusion barriers of around 1 eV are to be expected for ionically bonded nanoparticles on solid Xe in general.

The pre-exponential factor of the CdSe particle diffusivity on solid Xe, determined with the help of the diffusion-limited cluster-cluster aggregation Monte Carlo results,<sup>11</sup> was found to be  $10^{59} \text{ cm}^2/\text{s}$  for a particle of  $100 \text{ nm}^2$  projected area. (In BLAG, the prefactor scales as the inverse of the particle-buffer contact area).<sup>9</sup> It is many orders of magnitude higher than that of metal particles,<sup>11</sup> and it compensates for the increased effective barrier to result in comparable overall diffusivity. We previously explained the huge pre-exponential factors in particle slip-diffusion on surfaces with a statistical model that takes into account the multiphonon nature of diffusion excitation in estimating the entropy of the process.<sup>19</sup>

In order to probe the optical properties of the CdSe quantum dots, we measured PL spectra at 2 K under 457.9 nm (2.71 eV) excitation. Typical PL spectra are shown in Fig. 3, together with the corresponding particle size distributions. The particle sizes were obtained from TEM images as in Fig. 1, which were grown in parallel on standard TEM grids. In all cases, the peak signal appears at energies significantly higher than the low-temperature bulk band gap of 1.84 eV; indicating strong confinement.

The sample represented by Fig. 3(a) was produced from the deposition of 2 Å CdSe on 2 ML Xe, and was composed of a single layer of clusters with a mean diameter of  $\sim 3$  nm [see Fig. 1(a)]. It exhibits a strong PL peak at 2.60 eV, in very good agreement with results from colloidal CdSe particles of similar size.<sup>8</sup> In fact, a recent tight-binding calculation of the exciton energy shift in passivated II–VI nanoparticles predicts an energy of 2.66 eV for 3 nm particles,<sup>20</sup> and the difference can be accounted for by the spillover of the exciton wave function into the ZnS environment. By comparison with colloidal ZnS-coated CdSe particles, this difference is expected to be between 30 meV and 60 meV.<sup>8</sup>

The samples represented by Figs. 3(b) and 3(c) correspond to ramified islands with branch widths and heights of  $\sim 3$  nm. They demonstrate the transition from zero-dimensional to one-dimensional quantum structures. The sample in Fig. 3(b) was produced from the deposition of 1 Å CdSe on 12 ML Xe, and it exhibits a bimodal size distribution due to postdeposition fragmentation of the unstable branches during warm up to room temperature.<sup>10</sup> We attribute the PL peak at  $\sim 2.6$  eV to the clusterlike fragments, with sizes similar to the particles in Fig. 3(a). The size distribution peak at  $70 \text{ nm}^2$  of projected area can in first ap-

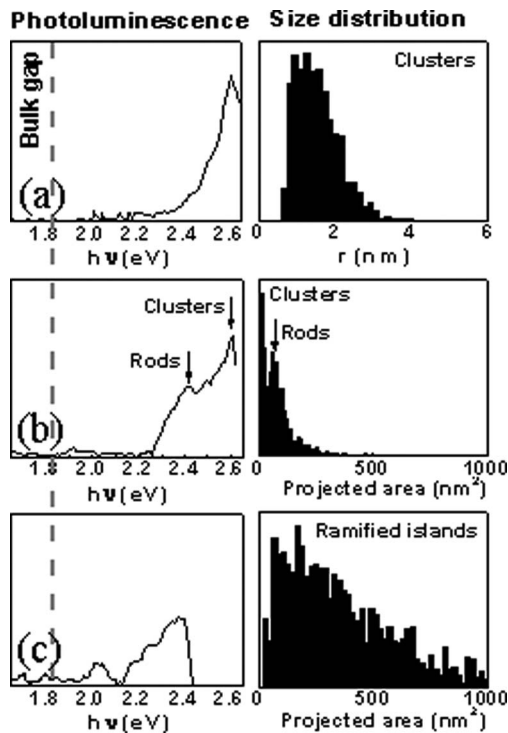


FIG. 3. PL signal from three representative samples measured at 2 K and the corresponding CdSe particle size distributions. Sample (a) consists of compact clusters of 1.5 nm mean radius, nucleated on a 2 ML Xe buffer. These exhibit a single PL peak at 2.6 eV. In (b) and (c), the clusters have aggregated during the desorption of thicker buffers to form rods and extended ramified islands, with typical branch widths of  $\sim 3$  nm. In (b), the branches have fragmented, and two distinct peaks are evident in both the size distribution and the PL response. The shift of the PL signal follows the transition from three- to two-dimensional confinement, but never reaches the bulk band gap (1.84 eV at 2 K), even for hundreds-of-nanometers-long islands as in the sample in (c).

proximation be attributed to  $\sim 23$  nm long rods. According to the empirical formula by Li *et al.*<sup>21</sup> (obtained from summarizing experimental data on colloidal CdSe rods), these should emit at 2.40 eV, which is in very good agreement with the lower-energy peak in the PL spectrum in Fig. 3(b), when corrected for temperature.

Further increase in projected area [as shown in Fig. 3(c), 2 Å CdSe on 18 ML Xe] corresponds to increase in the branch length and the number of branches in each island, but the average branch width is preserved at  $\sim 3$  nm. This leads to saturation in the PL shift toward lower energy, and bulk band-gap values are never reached, even by islands hundreds of nanometers long. Earlier effective mass approximation calculations have shown that the exciton gap in CdSe nanorods depends very weakly on rod length, for lengths significantly larger than the exciton Bohr radius,<sup>22</sup> which is 54 Å in CdSe. Significantly, this indicates that the electronic structure of these branches of limited length already exhibits one-dimensional character.

In summary, the rate of aggregation of the CdSe dots on solid Xe was investigated, and particle diffusion was found to reflect the existence of permanent dipoles on the particle

surfaces, exhibiting an effective diffusion activation energy about twice that observed previously for metal nanostructures. Photoexcited carriers in the CdSe dots exhibited strong quantum confinement, and PL measurements tracked the transition between three- and two-dimensional confinement as the particle morphology changed from compact to ramified. These results demonstrate that BLAG is applicable for the atomically clean synthesis of quantum dots and rods of II–VI semiconductors on almost any substrate. In particular, the method is compatible with the silicon technology, and it opens the door for the synthesis of optoelectronic nanodevices, such as ultraviolet/visible range quantum dot lasers and high-efficiency solar cells.

This work was supported by the U.S. Department of Energy Division of Materials Sciences under Grant No. DEFG02-01ER45944. The TEM imaging was carried out in the Center for Microanalysis of Materials, and PL measurements were done in the Laser and Spectroscopy Facility of the Frederick Seitz Materials Research Laboratory, which is partially supported by the U.S. Department of Energy under Grant No. DEFG02-91-ER45439. The authors thank A. S. Bhatti and S. G. Bishop for stimulating discussions.

<sup>1</sup>A. P. Alivisatos, *Science* **271**, 933 (1996).

<sup>2</sup>C. B. Murray, C. R. Kagan, and M. G. Bawendi, *Science* **270**, 1335 (1995).

<sup>3</sup>R. Bernard, G. Comtet, D. Dujardin, V. Huc, and A. J. Mayne, *Appl. Phys. Lett.* **87**, 053114 (2005).

<sup>4</sup>K. Walzer, U. J. Quaade, D. S. Ginger, N. C. Greenham, and K. Stokbro, *J. Appl. Phys.* **92**, 1434 (2002).

<sup>5</sup>M. Di Ventra, S. T. Pantelides, and N. D. Lang, *Phys. Rev. Lett.* **84**, 979 (2000).

<sup>6</sup>L. Huang, S. J. Chey, and J. H. Weaver, *Phys. Rev. Lett.* **80**, 4095 (1998).

<sup>7</sup>K. Yoo, A.-P. Li, Z. Y. Zhang, H. H. Weitering, F. Flack, M. G. Lagally, and J. F. Wendelken, *Surf. Sci.* **546**, L803 (2003).

<sup>8</sup>B. O. Dabbousi, J. Rodriguez-Viejo, F. V. Mikulec, J. R. Heine, H. Mattoussi, R. Ober, K. F. Jensen, and M. G. Bawendi, *J. Phys. Chem. B* **101**, 9463 (1997).

<sup>9</sup>V. N. Antonov, J. S. Palmer, A. S. Bhatti, and J. H. Weaver, *Phys. Rev. B* **68**, 205418 (2003).

<sup>10</sup>V. N. Antonov and J. H. Weaver, *Surf. Sci.* **526**, 97 (2003).

<sup>11</sup>V. N. Antonov, J. S. Palmer, P. S. Waggoner, A. S. Bhatti, and J. H. Weaver, *Phys. Rev. B* **70**, 045406 (2004).

<sup>12</sup>E. Rabani, B. Hetényi, B. J. Berne, and L. E. Brus, *J. Chem. Phys.* **110**, 5355 (1999).

<sup>13</sup>J. K. Nagle, *J. Am. Chem. Soc.* **112**, 4741 (1990).

<sup>14</sup>B. E. Sernelius, *Surface Modes in Physics* (Wiley-VCH, Berlin, 2001).

<sup>15</sup>S. H. Wemple, *Phys. Rev. B* **7**, 4007 (1973).

<sup>16</sup>J. C. Phillips, *Bonds and Bands in Semiconductors* (Academic, New York, 1973).

<sup>17</sup>G. Vidali, G. Ihm, H.-Y. Kim, and M. W. Cole, *Surf. Sci. Rep.* **12**, 135 (1991).

<sup>18</sup>J. L. F. Da Silva, C. Stampfl, and M. Scheffler, *Phys. Rev. Lett.* **90**, 066104 (2003); R. D. Diehl, Th. Seyller, M. Cargiu, G. S. Leatherman, N. Ferralis, K. Pussi, P. Kaukasoina, and N. Lindroos, *J. Phys.: Condens. Matter* **16**, S2839 (2004).

<sup>19</sup>A. Yelon and B. Movaghar, *Phys. Rev. Lett.* **65**, 618 (1990); G. Boisvert, L. J. Lewis, and A. Yelon, *ibid.* **75**, 469 (1995).

<sup>20</sup>S. Sapra and D. D. Sarma, *Phys. Rev. B* **69**, 125304 (2004).

<sup>21</sup>L.-S. Li, J. Hu, W. Yang, and A. P. Alivisatos, *Nano Lett.* **1**, 349 (2001).

<sup>22</sup>D. Katz, T. Wizansky, O. Millo, E. Rothenberg, T. Mokari, and U. Banin, *Phys. Rev. Lett.* **89**, 086801 (2002).